Journal of Food Composition and Analysis 145 (2025) 107764

Contents lists available at ScienceDirect

Journal of Food Composition and Analysis

journal homepage: www.elsevier.com/locate/jfca

Determination of phthalate esters released from prepared food packaging microplastics by nanoscale grafted silica based fabric phase sorptive extraction

Nasrin Moradi [a], Delaram-Sadat Tavoussi-Shirazi [a], Amir Mahdi Moshfegh [a], Abuzar Kabir [b], Habib Bagheri [a,*]

[a] Environmental and Bio–Analytical Laboratories, Department of Chemistry, Sharif University of Technology, P.O. Box 11365-9516, Tehran, Iran
[b] Department of Chemistry and Biochemistry, Florida International University, Miami, FL, USA

ARTICLE INFO

Keywords:
Fabric phase sorptive extraction
Nanoscale carbon
Microplastics
Phthalate esters

ABSTRACT

Microplastics have raised significant environmental and health concerns due to their widespread contamination. This study investigates the release of phthalate esters (PAEs) from microplastics using a fabric phase sorptive extraction method, prepared through silylation and grafting of nanoscale carbons to the fabric. The optimized method showed detection limits ranging from 0.003 to 0.01 ng mL^{-1}, a linear range of 0.01–800 ng mL^{-1} , and recovery values between 84.9 % and 101.2 % (RSD < 7.3 %) for PAEs extraction. The release behavior of phthalates from polystyrene microplastics was evaluated under various conditions, including aging and exposure to different environments (water and milk). Aging increased PAEs release by 2.8–4.5 times. When milk as the environmental matrix effect player was considered, dimethyl phthalate release decreased (~1.8 ×), while benzyl butyl phthalate increased (~2 ×), likely due to polarity differences. Additionally, the release of PAEs from four types of food packaging materials (polystyrene, polyethylene terephthalate, high-density polyethylene, and polypropylene) was examined, with benzyl butyl phthalate reaching up to 104.5 ng mL^{-1} in milk. The results show that while different quantities of phthalates were found in the containers, the release rates varied depending on the type of microplastics.

1. Introduction

Over recent years, microplastics (MPs) have caused a global environmental/health concern. MPs are regarded as the widespread and hazardous pollutants, defined as plastic particles smaller than 5 mm (Cao et al., 022). They can be primary MPs produced intentionally within this size range or secondary MPs due to the degradation of more oversized items in plastic (Xia et al., 2022). Among acrylics, polyesters, silicones, polyethylene, polypropylenes, polyurethanes, and halogenated plastics, polystyrene (PS), due to its lightweight and thermally insulating character, widens its use in food packaging and food containers. Meanwhile, the ability of PS MPs to release toxic additives, especially phthalate esters, into the food matrix poses a severe health threat (Ghoshal et al., 2023).

Phthalates (PAEs) are a group of chemical ingredients commonly added to impart elasticity and durability to many consumer products, including toys, food packaging, medical equipment, and personal care items (Yang et al., 2025). Yet, possible health effects from PAEs exposure cause serious concern, especially with so much approved scientific evidence. Apart from reproductive toxicity, developmental anomalies, and hormonal interference, PAEs have also been linked to obesity, asthma, and certain kinds of cancer (van 't Erve et al., 2019; Yang et al., 2025). Owing to their interfering effects on average growth and development, PAEs pose a specific threat to children, teenagers, and unborn infants. The PAE levels must be accurately quantified and monitored since phthalate plastics are pervasive in the environment and can bioaccumulate in human tissue (Yang et al., 2025). It is anticipated that release from plastics is the most crucial source of PAEs environmental pollution due to the non-covalent binding to polymers (Abdar et al., 2023). This is especially true for MPs, with an increased specific surface area. Considering the global pollution of MPs and frequent detection of PAEs in the environment (Cao et al., 2022), the behavior and mechanism of PAEs leaching from plastics and MPs are highly important. Although the release of PAEs from MPs under the influences of light, bacterial, and

* Corresponding author.
E-mail address: bagheri@sharif.edu (H. Bagheri).

https://doi.org/10.1016/j.jfca.2025.107764
Received 11 February 2025; Received in revised form 29 April 2025; Accepted 10 May 2025
Available online 14 May 2025

hydrostatic pressure has been reported, data related to the leaching behaviors of PAEs under other possible environmental conditions are not sufficiently available (Paluselli et al., 2019). It is highly important to determine the level of PAEs and, at the same time, to be able to monitor, especially in matrices like food, water, and consumer products, using accurate and sensitive analytical methods (Yang et al., 2025).

Sample preparation is usually essential in the analysis of PAEs in order to extract and eliminate matrix interferences (Behbahan et al., 2024). The most frequently used sample preparation techniques in the determination of PAEs include liquid-liquid extraction and solid-phase extraction, which are time-consuming, require a high quantity of organic solvents and are difficult to automate (Amritha et al., 2022). To overcome these disadvantages, different liquid-phase and sorbent-based microextraction techniques have been developed over the last decades. Fabric-phase sorptive extraction (FPSE), liquid phase microextraction (LPME), solid-phase microextraction (SPME), capsule-phase microextraction (CPME), stir bar sorptive extraction (SBSE), and pipette-tip solid-phase extraction (PT-SPE) are some typical micro-oriented techniques to resolve the existed problems. These techniques fulfill many general principles of green analytical chemistry (GAC) relevant to the organic solvent reduction and sample consumption (Bhadange et al., 2024; Tartaglia et al., 2022). The current study was conducted to examine the release of PAEs from PS MPs by developing an FPSE method.

The first proposal of the FPSE, as a promising and versatile sample preparation technique, was introduced a decade ago (Kumar et al., 2014). This technique resulted in improved extraction efficiency and selectivity due to the usage of organic/organic-inorganic hybrid polymer, the organically modified inorganic precursor(s), and the adsorptive nature of the fabric substrate. Since then, several forms of FPSE sorbents, such as neutral, cation or anion exchangers, mixed-mode exchangers, and zwitterionic ones, have been prepared and used to isolate different types of analytes from complicated matrices (Kabir & Samanidou, 2021; Moradi et al., 2023). The advantages of FPSE are ease of handling, rapid extraction kinetics, and high extraction efficiency, while it possesses various environment-friendly features (Tartaglia et al., 2022). Recent applications of FPSE have further demonstrated its versatility. For instance, a sol-gel FPSE method was applied to extract non-volatile plastic additives, such as diethyl phthalate, from food packaging materials, showing isolation of analytes with varying polarities. Three FPSE media coated with different sol-gel sorbents characterized with different polarities, including sol-gel based poly(dimethylsiloxane), poly (ethylene glycol) and poly(tetrahydrofuran), were studied (Aznar et al., 2016). FPSE combined with gas chromatography-mass spectrometry (GC-MS) was developed for the determination of emerging pollutants, including diethyl phthalate and dibutyl phthalate, in aqueous samples, proving its utility in environmental monitoring (Kaur et al., 2019). More recently, a universal sol-gel sorbent for FPSE was introduced, capable of extracting both polar and nonpolar compounds, including PAEs, demonstrating high selectivity and reproducibility, with applications in beverages, juices, and environmental samples (Olayanju et al., 2024). In this approach, we adapted the sol-gel approach, at the same time, to increase the durability and functionality of the fabric and to be able to graft the desired nanoparticles within the fabric structure. The sol-gel modified fabrics were subsequently coated with carbon nanotubes (CNTs), to conduct our research toward higher sorption capacity due to their unique structural properties. Incorporating CNTs increases the surface area available for interaction, enabling more efficient capture of organic compounds through strong π-π interactions and hydrogen bonding (Torabi et al., 2024). This modification not only enhances the extraction efficiency but also allows for reduced solvent consumption and shorter extraction times. The use of CNT-modified fabric films in FPSE represents a promising strategy for improving the sensitivity and reliability of analytical techniques, making it an effective tool for a wide range of applications in environmental monitoring, food safety, and chemical analysis.

This study presents a novel approach by modifying a fabric phase film with epoxy silane precursor using sol-gel methodology to enhance its durability. In a further step, CNT nanoparticles were chemically attached to the fabric surface, significantly improving the film's efficiency for extraction applications. Three PAEs (dimethyl phthalate, diethyl phthalate, and benzyl butyl phthalate) were selected for this study as model analytes due to their different polarities, which allowed us to assess both method effectiveness and matrix impact. This modified sorbent was used to extract PAEs from both water and milk matrices, making it possible to directly compare the effects of different matrices without the need for additional steps. Furthermore, the impact of the milk matrix, including its fat and protein content, on the release behaviors of MPs was investigated. The study investigates the release of PAEs from prepared MPs of food packaging plastics, such as those from commercial dairy containers. Considering the release of plastic additives from MPs released from the plastics, equivalent to 0.1–5 g per week (Senathirajah et al., 2021), which justifies the need to monitor such substances in daily food packaging. To our knowledge, this is the first study to investigate the direct effects of a milk matrix on the release behavior of MPs, and the use of CNT nanoparticles chemically attached to the fabric surface enhances the traditional sol-gel modification of the fabric for extraction applications. Thus, this study provides new insights into the interactions between food matrices and plastic additives, which could have significant implications for food safety and environmental health.

2. Experimental

2.1. Materials and methods

Organosilicon reagents, including [3-(2,3-epoxypropoxy)-propyl]-trimethoxysilane (Epoxy) and tetramethyl orthosilicate (TMOS) were obtained from Sigma-Aldrich (St. Louis, MO, USA). COOH Functionalized Multi-walled carbon nanotubes (COOH-CNTs) (>95 %, OD: 20–30 nm) were purchased from US Research Nanomaterials Inc. Dimethyl phthalate (DMP) (≥99 %), diethyl phthalate (DEP) (99.5 %), benzyl butyl phthalate (BBP) (98 %), polystyrene (PS) (Mw: 192000), triphenylphosphine (PPh_3), trifluoroacetic acid (TFA) and tetrahydrofuran (THF) were obtained from Sigma-Aldrich (St. Louis, MO, USA). Ethyl acetate was purchased from Daejung Chemicals (Korea). Methanol (MeOH) solvent utilized in this study was sourced from Baher Exir Kaveh, located in Saveh, Iran, and is of GC-grade quality. Stock solutions of DMP, DEP, and BBP were prepared in GC-grade MeOH at a concentration of 1000 mg L^{-1} and stored at 4 °C. Working solutions were freshly prepared daily from the respective stock solutions by dilution with deionized water. To enhance the analytical signal and the extraction efficiency, the effective parameters in the extraction and desorption process were considered to be optimized. Optimization covered the type and amount of the desorption solvent, and the extraction/desorption time, respectively. All the optimization steps were performed at a concentration of 0.5 mg L^{-1} in triplicate. Before analysis, all milk samples were diluted ten times using deionized water and stored at 4 °C.

2.2. Instrumentation

Optimization of the synthesis and extraction process was conducted using a gas chromatograph model Agilent 6820, featuring a split/splitless injection port and a flame ionization detection system. A medium bore HP-5 MS column (Hewlett−Packard, Palo Alto, CA, USA, 30 m × 0.32 mm i.d. and 0.25 μm film thickness) was proved to be a suitable platform for separating the desired analytes. Nitrogen gas with a purity of 99.999 % was utilized as the carrier gas, with flow rates of 1 mL min^{-1}. Sample introduction was carried out in splitless mode, with the split valve closed for 2 min. The injector and detector temperatures were both maintained at 280 °C.

A Hewlett-Packard (HP) 6890 series gas chromatograph (Palo Alto,

California, United States) was utilized for the analysis of real samples and conducting quantitative surveys. This system was connected to an HP 5973 mass-selective detector. The mass spectrometer operated under electron ionization (EI) mode at 70 eV while helium (99.999 %) carrier gas adjusted at 1 mL min^{-1}. Controlled temperatures were crucial for optimal performance: the GC–MS interface, ion source, and mass analyzer were set to 280, 230, and 150 °C, respectively. Regarding the chromatographic process, the column's initial temperature was set at 100 °C and maintained for 3 min before ramping up to 280 °C at 40 °C min^{-1}. Injection occurred in the splitless mode for ~~3~~ 2 min while it was set at 280 °C. To enhance sensitivity for each individual compound, a time-scheduled selected ion monitoring (SIM) mode was implemented, focusing on mass peaks of the highest intensity. This approach aimed to maximize detection efficiency and accuracy in compound identification. The retention times and selected masses for each individual analyte are tabulated in Table S1. Fourier transform infrared (FTIR) spectroscopy analysis, Perkin Elmer Spectrum 1 (4000–400 cm^{-1}) with ATR accessory, and ABB Bomem (MB100 model, Quebec, Canada) spectrometer, were used to identify functional groups on the fabric surface and to examine of MPs surface after aging, respectively. A field emission scanning electron microscope (FE-SEM) (MIRA3 TESCAN, www.tescan.com) was used to examine the surface morphology of the MPs surface and the fabric before and after modification by COOH-CNT. A Philips PW1730 was used for X-ray diffraction (XRD) analysis of modified fabrics. The surface aging of MPs was carried out using a home-made array of UV LED lamps emitting at 265 nm. The irradiation system, powered by a 12 V/5 A adapter, was positioned 10 cm above the Petri dish containing MPs. Detailed technical specifications of the lamp and the experimental setup are provided in the Supplementary Material. Additionally, the schematic illustration of the setup is shown in Fig. S1 to demonstrate the spatial arrangement of the UV source and the MPs during irradiation. Elmasonic S ultrasonic bath (Germany) was utilized for grafting the CNT on the fabric surface. All deionized water was used from the ultrapure water system of ZU101-C Zolalan Company. Biosan Multi-Vortex V-32 (Latvia) was applied for the performing desorption process. A magnetic hot plate stirrer (IKA RH Basic 2) was used for extraction and releasing processes.

2.3. Preparation of MPs

In the present study, the release of PAEs (DMP, DEP, BBP) from PS MPs was investigated (the physicochemical properties of studied phthalates are listed in Table S2). To prepare the PS MPs, the PS beads were dissolved in THF. Then, a homogeneous solution of 10 % (*w/v*) PS was prepared by sonication. This solution was cast on a Petri dish, and subsequently, the solvent was evaporated under ambient conditions. The obtained PS film was cut into small fragments by scissors and then ground with the electrical mill under liquid nitrogen media. The size of the PS MPs was assessed by passing them through mesh screens, and the particles were 420–700 μm in size. For the preparation of MPs containing plasticizers, PAEs were fortified to the dissolving process at a specified ratio of PAEs/PS (1/10). A homemade UV lamp was employed to age the PS MPs for a duration of 50 h.

Real plastic samples were collected from the daily used items, including milk bottles, cheese and cream containers, disposable food containers and coffee cups, made of polystyrene (PS), polyethylene terephthalate (PET), high-density polyethylene (HDPE), and polypropylene (PP). The plastics were washed with deionized water, then dried, cut into smaller pieces with scissors, and then ground to produce MPs. The size of the ground MPs from these real plastic samples was controlled by mesh screening, resulting in particles between 420–700 μm. The PET bottle and PS disposable food container were cut into small pieces only with scissors. The produced MPs were larger and ranged between 1000–1410 μm.

2.4. Leaching experiments

First, all glass containers were treated with chromic acid to oxidize organic contaminants, followed by washing with deionized water. The release conditions for PS MP samples prepared from polystyrene film with the addition of PAEs were investigated for aged PS MPs and in different environments of water and milk. Experiments on releasing PAEs from PS MPs were carried out in glass bottles by adding a specific mass of MPs (0.015 g) to a particular volume of water or milk (20 mL). This concentration was simulated considering the minimum daily ingestion rates of MPs, which have been estimated to be in the range of 0.1–5 g for a week (Senathirajah et al., 2021). Accordingly, the tubes were highly agitated utilizing a magnetic stirrer. Every experimental condition was run in triplicate to ensure the repeatability of the results. To inhibit microbial degradation, all solutions were made with the addition of sodium azide (400 mg L^{-1}). Various experimental conditions, including aging effects, and the influence of a milk food matrix, were examined. This was based on the previous study showing that the influence of salt concentration and pH on the leaching processes is negligible (Gulizia et al., 2023). The fortification of PAEs into the milk matrix was achieved by the tenfold dilution of the samples with deionized water.

For PAEs release from MP samples prepared from real food packaging containing dairy products available on the market, only a higher amount of MPs (0.1 g) was used under the same release conditions as the PS MP samples.

2.5. Modification of fabric phase

2.5.1. Pre-treatment of fabric substrate

The cellulose fabric was immersed in 1 % solution of the non-ionic detergent in deionized water, heated to 50 °C for 30 min to clean and remove the surface impurities. Subsequently, the fabric was washed thoroughly using deionized water and allowed to air dry at room temperature. Pieces of cellulose fabric were cut and washed with deionized water. Then, the fabric surface was activated by immersing it in a 1 M sodium hydroxide solution for 1 h. To remove the bases, cellulose fabrics were further washed with deionized water several times, followed by treatment in a 0.1 M HCl solution for 1 h. The fabric was then air-dried and put in a clean container for future use.

2.5.2. Fabric surface modification using sol-gel method

For the implementation of the sol-gel approach, a sol solution was prepared by adding 6 mL of Epoxy and TMOS as sol-gel precursors at ratios of 1:1, 5:1, and 6:0 while 2 mL of TFA, as a catalyst, was added to 20 mL of dichloromethane/acetone at a 1:1 ratio. A piece of fabric was immersed in the sol solution for 2 h. Then, the top solution was drained, and the sol-gel on the fabric surface was aged at 50 ° C for 4 h. Afterwards, the fabric was washed with enough water. The schematic of functionalizing cotton fabrics using the sol-gel method is shown in Fig. 1a.

2.5.3. Integration of CNTs into sol-gel epoxy coated fabric

The fabric treated with epoxy groups was suspended inside THF solvent container. 60 mg of COOH-CNTs and 15 mg of PPh_3 were added to the reaction bottle and placed in an ultrasonic bath at the 55 °C temperature for 15 min. The modified fabric was removed from the solution, washed with deionized water and ethanol, and dried at ambient temperature. Schematic illustration in Fig. 1b showed the structural mechanism responsible for the attachment of COOH-CNTs on the functionalize cotton fabric surface (Guadagno et al., 2019). To complement the schematic representation, Fig. 1c–h present the photographic images of the actual synthesized sorbents prepared using different ratios of sol–gel precursors and varying amounts of CNTs. These images provide visual confirmation of the effect of synthesis parameters on the surface appearance of the final sorbent materials.

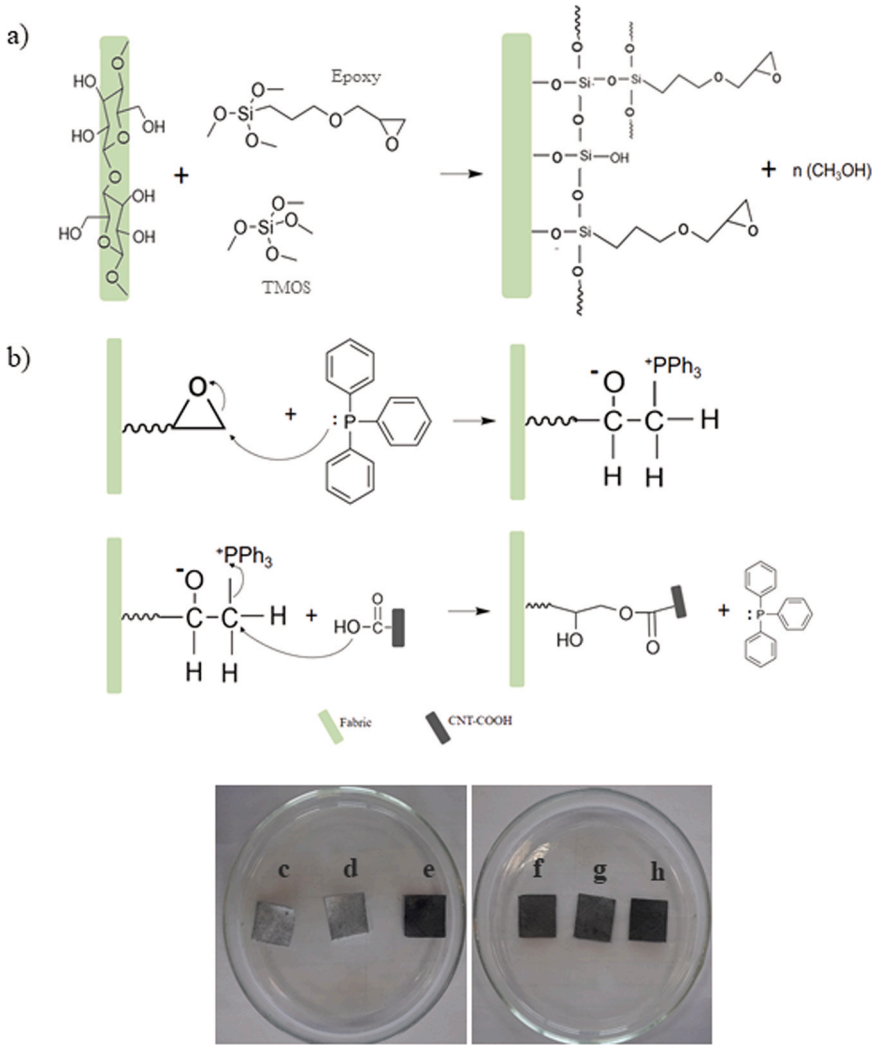

Fig. 1. Schematic illustration of a) functionalizing cotton fabrics using the sol-gel method, and b) the structural mechanism responsible for the attachment of carbon nanotubes (CNTs) on the functionalized cotton fabric surface. Photographs of the modified fabrics with different sol-gel precursor ratios and CNT amounts: c) CNT (60 mg) - Epoxy/TMOS (1:1) - Fabric, d) CNT (60 mg) - Epoxy/TMOS (5:1) -Fabric, e) CNT (60 mg) - Epoxy - Fabric, f) CNT (40 mg) - Epoxy - Fabric, g) CNT (50 mg) - Epoxy - Fabric and h) CNT (60 mg) - Epoxy – Fabric.

2.6. The FPSE procedure

The prepared fabric was cut into 1 cm^2 pieces. A piece of modified fabric was inserted into 7 mL of the sample solution of PAEs at 0.5 mg L^{-1}, attached *via* a wire, and the extraction process was performed within 15 min, with agitation provided by a magnetic stirrer. Then, the fabric was removed from the sample solution, washed with deionized water. For desorption, the fabric was inserted into a microtube containing 500 µL of ethyl acetate and vortexed for 10 min. The desorption solvent was evaporated under a stream of nitrogen gas. Finally, the remaining analytes were dissolved in 20 µL of MeOH, of which 1 µL was injected into the GC system.

2.7. Reusability

To study the reusability of the fabric coated with CNT, FPSE procedure experiments were carried out using 7 mL of testing solution at 0.5 mg L^{-1} in the milk matrix. After 15 min of adsorption, the fabric was removed and put into a microtube containing 500 µL of desorption solvent to elute the analytes. This adsorption-desorption cycle was repeated several times. The amount of the analytes extracted was measured after each cycle.

3. Results and discussions

3.1. Characterization of CNT-epoxy fabric film

In order to obtain information about the degree of crystallinity of cellulose fabric and modified fabrics, XRD analysis was performed (Fig. 2a-c). Typical diffraction peaks at $2\theta = 15.2$, 16.7, 22.8, and 34.7° are seen in the diffraction patterns, which correspond to the crystal lattices in the native cellulose structure (Acharya et al., 2021). These results in Fig. 2b indicate that the crystallinity is reduced due to the amorphous regions of sol-gel, and the type of cellulose crystal does not alter much in this modification step.

Fig. 2c reveals that the intensities of the peaks have been reduced, and this could be due to the grafting of the CNTs at thermal and sonication condition that partially destroys the structure of cotton fibers. However, the XRD pattern of the fabric substrate is preserved (Chen et al., 2021). Adding CNTs into cotton fabric does not affect the crystalline structure of the parent material. With CNTs coated onto the fabric, the diffraction peak attributed to CNTs becomes less intense due to their lower fraction than cellulose (Chen et al., 2021; Costa et al., 2020; Maity et al., 2021).

The attenuated total reflectance - Fourier transform infrared (ATR-

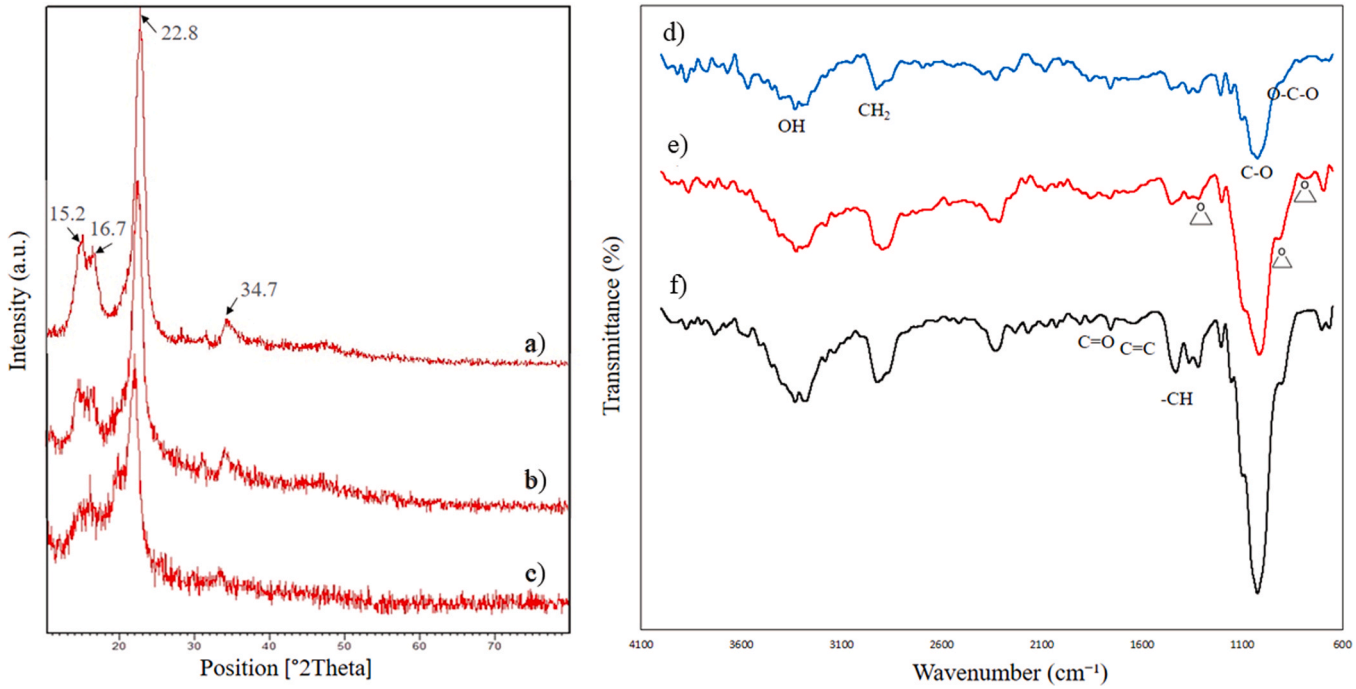

Fig. 2. X-ray diffraction (XRD) pattern of a) pristine cotton fabric, b) epoxy fabric, c) carbon nanotubes (CNTs) coated with sol–gel-based fabric, and attenuated total reflectance - Fourier transform infrared (ATR-FTIR) spectra of d) pristine fabric, e) epoxy coated fabric, and f) CNT coating.

FTIR) spectra of original cotton fabric, sol-gel coated fabric, and CNT/sol-gel coating fabric are shown in Fig. 2d-f. For uncoated fabric, the peaks at 3600–3300, 3000–2800 and 1000 cm^{-1} were assigned to the stretching vibration of O–H, C-H, and C-O, respectively (Li et al., 2018). For sol-gel coated fabric, the absorption peaks at 782, 910, and 1210 cm^{-1} are attributed to the epoxy functionalized group in the sol-gel structure. The bands at 1631, 3327, and 1432 cm^{-1} confirm the presence of the stretching vibrations of C═C, -CH, and bending of –CH in CNT. For CNT/epoxy sol-gel fabric, the Si–O in the sol-gel network overlaps with the C-O bond in the same regions at 1100 cm^{-1}. Also, the peaks at 1000–1200, 1743, and 3400 cm^{-1} are attributed to the presence of C-O, C═O and –OH stretching vibrations of carboxylic groups in CNT (Lu et al., 2022).

FE-SEM images were obtained in order to investigate the fabric surface morphology. The raw fabric surface initially was smooth and without protrusions, as shown in Fig. 3a, b. However, according to Fig. 3c, the sol-gel fabric shows some degree of roughness, appearing on the fabric surface. More importantly, as shown in Figs. 3d and 3e, the presence of CNTs is rather evident.

Energy Dispersive Spectroscopy (EDS) analysis was employed to verify if any elemental change had occurred at the surface after it was subjected to treatment with the sol-gel method and CNTs grafting. The corresponding FE-SEM image and EDS mapping are shown in Fig. 3f, g. The cotton fabric, with carbon and oxygen elements, contains Si after the sol-gel treatment. Similarly, the CNTs used in the subsequent step are made up of carbon and oxygen, just like the elemental mapping of the original fabric.

3.2. Aged MPs characterization

Aging in MPs causes alteration in the surface roughness, functional groups on the surface, and, in fact, changes in hydrophilic property and crystallinity. All that eventually changes the behavior of adsorption and release of organic pollutants from MPs. For PS, the change in crystallinity is not related to the adsorption capacity of organic compounds because of its low level of crystallinity (Yan et al., 2021). By comparing the FE-SEM images of MPs appearing in Fig. 4 before and after aging, an increase in fractured areas can be observed. Testing for the change in functional groups shows that functional groups containing oxygen on the surface of plastic increased after the aging process, as shown in Fig. 4g-i. The areas related to C-O and C═O bonds in the relevant PAEs, as shown in Fig. 4h, lead to more intense peaks in aged MPs (Fig. 4i).

3.3. Optimization

3.3.1. Optimization of extractive film synthesis

The optimization of the extractive film synthesis focused on modifying the fabric substrate to enhance the sorption capacity. Initially, the unmodified fabric demonstrated low extraction efficiency for selected PAEs 0.2 %, 0.3 % and 0.4 % for DMP, DEP, and BBP, respectively (Fig. 5a). Surface modification with sol-gel precursors, including silane compounds (Epoxy/TMOS, 1:1), improved the sorption process by creating a sol-gel structure, which enhanced interactions between the fabric and the PAEs (2.2 %, 2.2 % and 3.1 % for DMP, DEP and BBP, respectively). Further enhancement was achieved through the incorporation of CNTs, where the highest recoveries were obtained: DMP (5.9 %), DEP (5.4 %), and BBP (8.3 %). This improvement can be attributed to additional hydrogen bonding and π–π interactions facilitated by the presence of CNTs.

In this paper, we studied the synthesis of sol-gel-based sorbents using different precursor quantities. More precisely, the impact of varying the Epoxy and TMOS ratios, such as 1:1, 5:1, and 6:0, was considered. As a result, a specific interesting trend was obtained, which was illustrated in Fig. 5b. With increasing TMOS content, a structure with higher strength was obtained. However, subsequent steps did not yield a good grafting of CNTs to the surface. In contrast, in the absence of TMOS (Epoxy only), the fabric surface became visibly darker (Fig. 1c-e), and extraction efficiency increased significantly, reaching 32.4 % for DMP, 29.8 % for DEP, and 30.5 % for BBP—representing an improvement of over 4-fold compared to Epoxy/TMOS (1:1). This indicates that eliminating TMOS enhances CNT immobilization and overall sorbent performance.

The influence of CNTs content was also investigated. Increasing the CNT amount from 40 to 60 mg led to a significant improvement in extraction efficiency, as shown in Fig. 5c. For instance, recovery for DMP

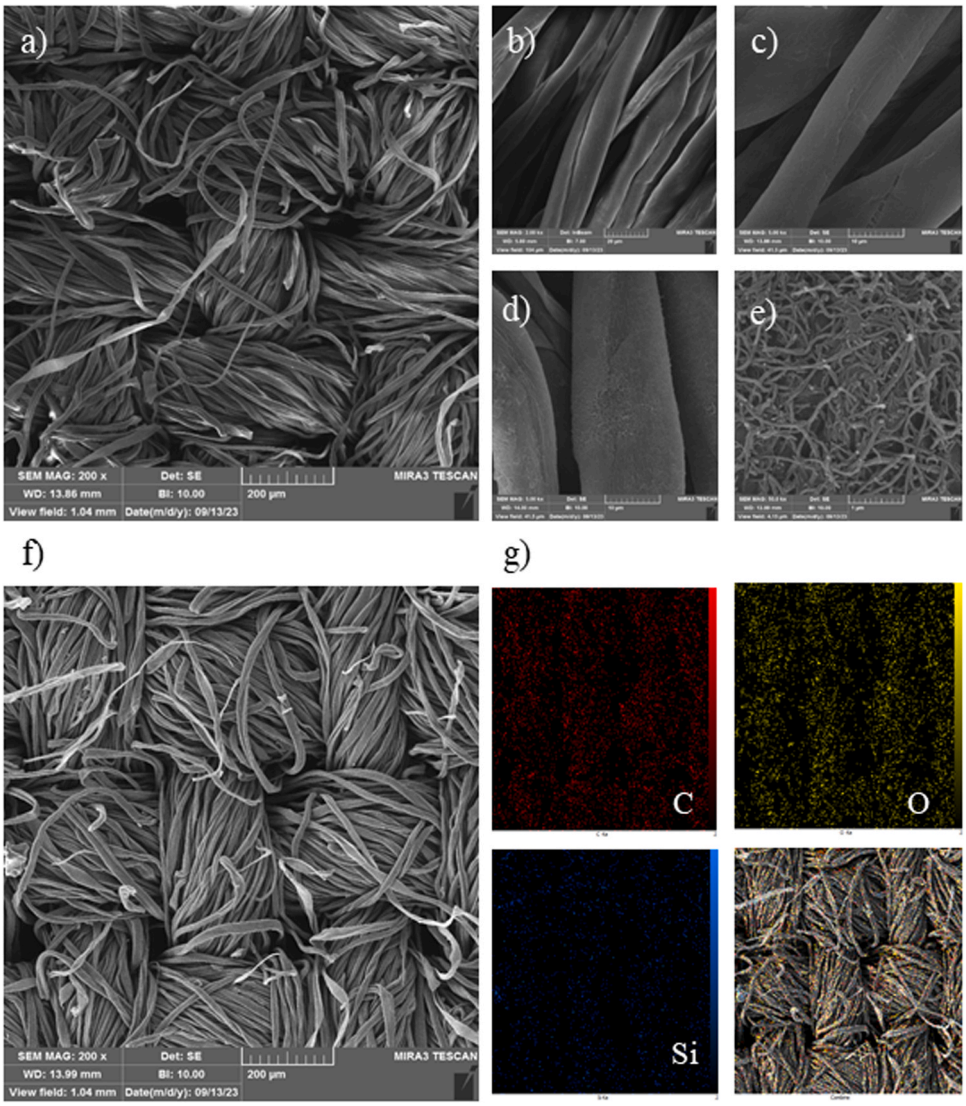

Fig. 3. Field emission scanning electron microscope (FE-SEM) images of a, b) pristine cotton fabric, c) epoxy fabric, d, e) carbon nanotubes (CNTs) coated with sol–gel-based fabric, f) FE-SEM image of CNTs coated with sol–gel-based fabric, and g) energy dispersive X-ray spectroscopy (EDS) element mapping.

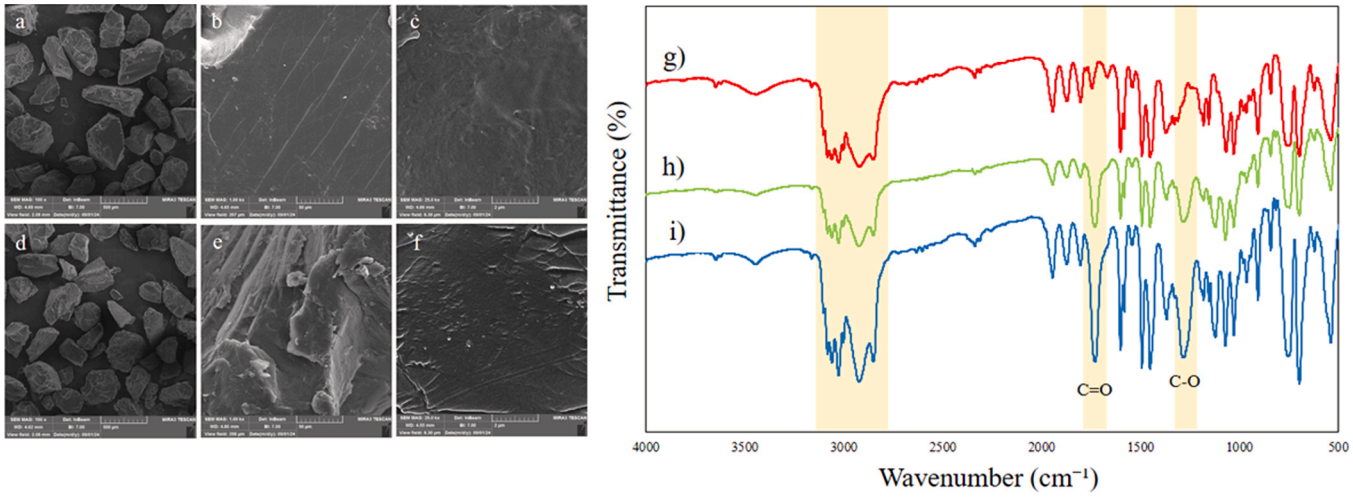

Fig. 4. Field emission scanning electron microscope (FE-SEM) images of a-c) polystyrene microplastics (PS MPs) + 10 % phthalate esters (PAEs), e-f) aged PS MPs + 10 % PAEs, and Fourier transform infrared spectra of g) pristine PS MPs, h) PS MPs + 10 % PAEs, and i) aged PS MPs + 10 % PAEs.

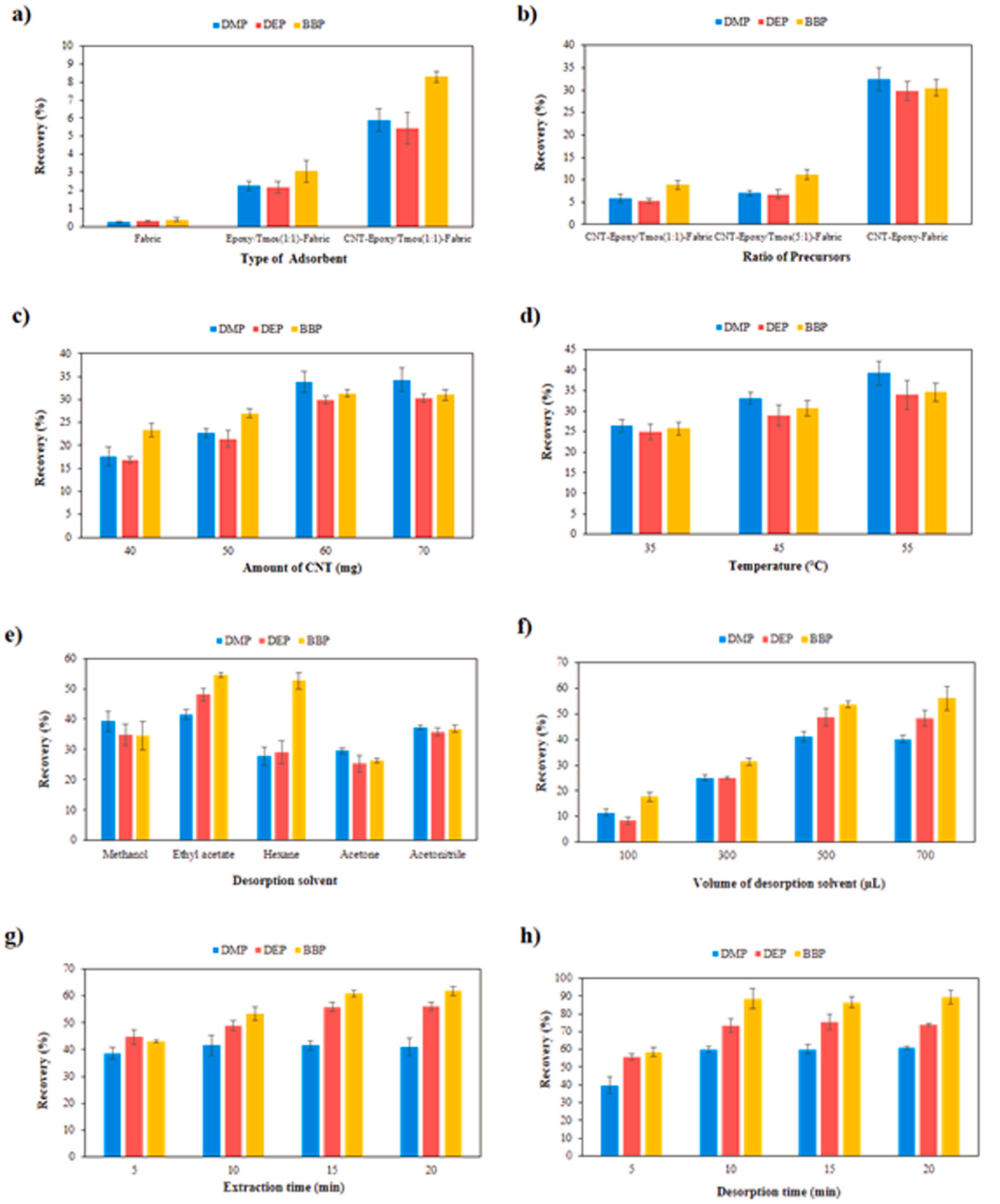

Fig. 5. Optimization: a) comparison of the adsorbents, b) ratio sol-gel precursors, c) amount of carbon nanotubes (CNTs), d) temperature conditions for grafting CNTs, e) type of desorption solvent, f) amount of desorption solvent, g) extraction time, and h) desorption time. (Dimethyl phthalate (DMP), diethyl phthalate (DEP), benzyl butyl phthalate (BBP)).

increased from 17.7 % (40 mg) to 33.9 % (60 mg), and similar trends were observed for DEP (16.9–29.9 %) and BBP (23.4–31.4 %). However, a further increase to 70 mg resulted in no noticeable improvement, indicating a plateau in sorption efficiency. Visually, higher CNT loadings produced darker fabrics (Fig. 1f-h), confirming increased surface coverage.

The effect of reaction temperature was also studied at 35, 45, and 55°C. At 55°C, a higher amount of CNTs was grafted to the surface. Temperatures above 55°C were avoided because higher temperatures in a sealed reaction vessel under ultrasonic conditions could lead to structural instability, potentially causing cracking, which is undesirable (Fig. 5d).

The statistical significance of the differences between each optimized value for extractive film synthesis parameters was evaluated using one-way analysis of variance (ANOVA) at $p < 0.05$. The results are summarized in Table S3. In each case, ANOVA was applied to compare the recovery efficiencies among different levels of the tested variables (e.g., different adsorbent types, precursor ratios, CNT amounts, and reaction temperatures). The significant p-values confirmed that the selected optimized conditions were statistically different to the alternative tested conditions, thus validating the reliability of the optimization process.

3.3.2. Optimization of extraction and desorption parameters

The selection of a suitable desorption solvent is essential for achieving optimum recovery. Various common solvents with differing polarities—methanol, ethyl acetate, hexane, acetone, and acetonitrile—were tested (Fig. 5e). Among them, ethyl acetate resulted in the highest extraction recoveries, with 41.5 % for DMP, 48.1 % for DEP, and 54.5 % for BBP. This improvement is likely due to structural compatibility between ethyl acetate and the phthalate esters, which facilitates more efficient desorption. By contrast, lower recoveries were observed with methanol (e.g., 39.2 % for DMP), and particularly with acetone and hexane, where DMP recovery dropped to 29.6 % and 27.8 %, respectively. Based on these results, ethyl acetate was selected as the desorption solvent for subsequent steps.

The desorbing solvent volume was varied from 0.1 to 0.7 mL to optimize extraction efficiency (Fig. 5f). Recoveries increased notably up to 0.5 mL (e.g., DMP: 11.4 % → 41.3 %), with only slight improvement beyond that. Thus, 0.5 mL was selected as the optimal volume due to its efficiency and minimal solvent use.

Extraction and desorption times were optimized based on recovery efficiency (Fig. 5g, h). Extraction recovery increased with time, reaching a maximum at 15 min (DMP: 42.4 %, DMP: 56.1 %, BBP: 60.9 %), with minimal change beyond that.

Similarly, desorption efficiency peaked at 10 min (DMP: 60.0 %, DEP: 73.5 %, BBP: 88.6 %), and longer times showed no significant improvement. Therefore, 15 min for extraction and 10 min for desorption were selected as optimal conditions. Similarly, the differences among the tested levels within each extraction and desorption parameter were statistically analyzed by one-way ANOVA based on a significance level of $p < 0.05$, confirming the selection of optimized conditions. Detailed results are provided in Table S3.

3.4. Reusability and stability of CNT/epoxy coated FPSE film

FPSE films provide advantages such as simplicity and low cost, but practical application requires sorbents with high sorption capacity, fast kinetics, and long-term durability—a key factor in extraction method design (Abdar et al., 2022). The reusability of the CNT/Epoxy-coated fabric was tested over 25 extraction cycles (Fig. S2). Recovery remained stable for up to 20 cycles, with values within 79–83 % of the initial use. After that, a gradual decline occurred due to the physical degradation of the fabric and a partial loss of CNT coating. These results support its applicability for at least 20 consecutive extractions without significant loss of performance. However, to ensure optimal performance in practical applications, the sorbent was not used beyond 5 extraction cycles in this study.

3.5. Analytical validation

A calibration curve for the selected PAEs in water samples was made under optimized conditions. According to Table 1, a linear range of 0.03–800 ng mL^{-1} for DMP and DEP, and 0.01–800 ng mL^{-1} for BBP with an appropriate correlation coefficient of 0.9895–0.9987 was obtained. The limits of detection (LOD, $S/N = 3$) ranged from 0.003 ng mL^{-1} (BBP) to 0.010 ng mL^{-1} (DMP and DEP), and limits of quantification (LOQ, $S/N = 10$) values of 0.01–0.03 ng mL^{-1} were achievable. The relative standard deviation (RSD) values for intra-day and inter-day precision were also satisfactory. For example, the intra-day RSDs at 1 ng mL^{-1} were 5.2 % (DMP), 3.4 % (DEP), and 4.1 % (BBP), while the inter-day RSDs at 200 ng mL^{-1} ranged from 6.8 % (DEP) to 7.2 % (BBP). The effect of extraction film variation on repeatability was also tested at 200 ng mL^{-1}, and the obtained RSD % values were 7.4 % for DMP, 7.9 % for DEP, and 8.1 % for BBP.

For milk samples, the calibration curves were constructed by spiking PAEs into the diluted blank milks (Table S4). The optimal conditions were applied to assess the efficiency of the developed extraction method in real tap water matrix and milk samples. Each sample was analyzed based on its own specific calibration curve. As presented in Table S5, for the spiked water and milk samples at 5 and 100 ng mL^{-1}, the relative recovery values of 84.9–101.2 % were obtained (RSD % 4.3–7.3 %). These results show that the developed method is effective in real matrices, including water and milk, and presents negligible matrix effects.

Our work outputs were compared with the results from other relevant studies (Alshehri et al., 2022; Hou et al., 2022; Huang et al., 2020; Keshavarzi et al., 2022; Yue et al., 2020), and as Table S6 demonstrate, the linear ranges, LODs, and RSDs% are all within the range and limits reported for the determination of PAEs in different matrices. The extraction time of 15 min is either lower or equal to the reported values, which may be because a fabric substrate was used in this study. This approach resembles dispersive extraction techniques, where the sorbent is distributed throughout the sample matrix, reducing the extraction time. This reduction can be explained by enhanced mass transport and facilitated penetration into the fabric fibers for effective extraction of the analytes.

3.6. Effects of influential parameters on PAEs release from PS MPs

MPs particle size, the concentration of PAEs, and media temperature are important features influencing the release rate. The studies have reported that a decrease in particle size, an increase in PAEs content, and a rise in temperature lead to higher release levels (Gulizia et al., 2023; Yan et al., 2021). In this study, the effects of aging and the milk matrix on the release behavior of PS MP were investigated.

3.6.1. Aging

Photooxidation through UV radiation, biodegradation, chemical oxidation, and physical treatment are contributing factors in the general processes through which plastic polymers and associated additives may enter the environment. The aging of MPs has a great effect on the rate of additive release, while natural aging takes decades or even centuries, artificial aging processes may take several days or months. Solar radiation is, therefore, highly involved in this process, as most MPs are regularly exposed to sunlight. Moreover, UV radiation affects the aging and release of additives from MPs. As confirmed by the other studies, UV exposure increases the release of organic pollutants encapsulated in MPs. It has been reported that the additive release rate upon light exposure becomes five times higher than the rates in darkness. Such an increase is caused by the continuous irradiation of light, which forms reactive oxygen species, such as hydroxyl radicals and superoxide anions, able to attack the chains of the polymer, thereby causing cleavage

Table 1
Analytical figures of merit obtained from the developed fabric-phase sorptive extraction (FPSE)-GC-MS method in water.

Analyte	Linear range (ng mL^{-1})	LOD[a] (ng mL^{-1})	LOQ[b] (ng mL^{-1})	Correlation coefficient (R^2)	Intra-day RSD[c]% (n = 5)		Inter-day RSD% (n = 5)		Batch to batch
					1 (ng mL^{-1})	200 (ng mL^{-1})	1 (ng mL^{-1})	200 (ng mL^{-1})	
Dimethyl phthalate	0.03—800	0.010	0.03	0.9902	5.2	4.9	6.1	7.1	7.4
Diethyl phthalate	0.03—800	0.010	0.03	0.9895	3.4	5.1	5.9	6.8	7.9
Benzyl butyl phthalate	0.01—800	0.003	0.01	0.9987	4.1	3.3	5.7	7.2	8.1

[a] Limit of detection
[b] Limit of quantification
[c] Relative standard deviation

and degradation of the polymer structure afterward (Li et al., 2024; Yu et al., 2024; Zha et al., 2022). In our study, the accelerated aging process led to a noticeable increase in the release of PAEs: for example, DMP increased from 169 to 601, DEP from 236 to 672, and BBP from 108 to 485 ng mL^{-1}, corresponding to an increase of ~3.6 × for DMP, ~2.8 × for DEP, and ~4.5 × for BBP. BBP exhibited the highest release enhancement, probably due to its greater hydrophobicity. The changes of the functional groups toward hydrophilic properties on the MPs surface reduce the affinity of PAEs to the plastic network (Fig. S3a).

3.6.2. Environment

The amount of dissolved organic matter (DOM) in the environment where the MPs are placed accordingly varies the pollutant sorption and release behavior (Liu et al., 2019). Studies show that an increase in DOM increases the solubility of more non-polar compounds, thereby increasing the release rate. On the other hand, the stronger affinity of these materials compared to pure water leads to better extraction of PAEs (Yan et al., 2021). To expand into real food matrices, an attempt was made to investigate the role of milk as a representative matrix for other fats and soluble proteins. Bovine milk is a natural and complex matrix, containing DOM primarily composed of proteins (caseins and whey proteins), lactose, lipids, and other small organic molecules; additionally, minerals are also present (Roy et al., 2020). These components significantly contribute to the DOM background and can influence the interaction and release behavior of pollutants. The PAEs released from MPs in diluted milk samples compared to water, are shown in Fig. S3b. DMP release decreased from 200 to 110 ng mL^{-1} in milk, while BBP increased from 103 to 184 ng mL^{-1}. Therefore, it could be deduced that the increase of DOM leads to an increase of more non-polar compounds in milk.

3.7. Real sample applications

To investigate the release of PAEs from MPs in different environments, four types of MPs prepared from different types of real food packaging plastics were selected. The amounts of PAEs released from these MPs in different products vary with each other, which is due to the different amount of PAEs used in each polymer type and their different affinity toward the plastic polymer. The analysis of four types of selected polymers led to the various amounts of investigated PAEs (Table 2). Among the plastics, the breakfast cream packaging PS showed the highest release with the total amounts of 178.5 (DMP: 70.3, DEP: 94.5, BBP: 13.7 ng mL^{-1}) in water and 195 ng mL^{-1} (DMP: 51.6, DEP: 78.9, BBP: 64.5 ng mL^{-1}) in milk. On the other hand, the disposable container PS released the lowest amount (54.3 and 40.5 ng mL^{-1}, in water and milk matrices, respectively). Among the studied PAEs, DEP and BBP were found in most types of polymers. The different amounts of released PAEs depend on the molecular size of the phthalates and their concentration in the plastic. As expected, the migration of smaller molecules, such as DMP and DEP, is more feasible, and DMP was detected mostly in PS and HDPE samples, with values up to 70.3 ng mL^{-1} . In the meantime, the amount of released BBP is higher in the milk environment, which is associated with the higher solubility of this phthalate in organic environments, and the possibility that the affinity of the molecules inside the milk tissue is greater than BBP to plastic.

4. Conclusions

In this study, an FPSE sorbent was fabricated by modifying a fabric substrate with epoxy-based sol–gel chemistry and further functionalizing it with CNT nanoparticles. This hybrid sorbent demonstrated high extraction efficiency for three model phthalates (DMP, DEP, BBP), showing rapid extraction kinetics (15 min), sufficient reusability (up to 20 cycles with ~80 % retention), and strong performance in real

Table 2
The leaching of phthalate esters (PAEs) (ng mL^{-1}) from different microplastics (0.1 g) made of commercial container food into water and milk matrices.

Polymer	Plastic product	Release matrix	Dimethyl phthalate		Diethyl phthalate		Benzyl butyl phthalate	
			Found amount (ng mL^{-1})	RSD[a](%)	Found amount (ng mL^{-1})	RSD(%)	Found amount (ng mL^{-1})	RSD(%)
PS[b]	Cream container	Water	70.3	5.7	94.5	8.0	13.7	10.2
		Milk	51.6	8.9	78.9	6.6	64.5	5.9
PS	Disposable food containers	Water	ND[c]	9.1	54.3	6.9	ND	6.4
		Milk	ND	5.1	40.5	7.8	ND	8.1
PET[d]	Milk bottle	Water	ND	4.9	77.4	10.6	4.2	4.8
		Milk	ND	7.7	69.7	11.3	21.0	9.5
HDPE[e]	Milk bottle	Water	66.9	6.5	73.8	9.2	5.2	8.7
		Milk	41.5	8.5	70.4	9.8	19.8	10.3
PP[f]	Coffee milk cup	Water	ND	9.4	ND	6.8	29.1	5.8
		Milk	ND	10.2	ND	10.6	67.0	6.9
PP	Cheese container	Water	ND	6.7	63.8	10.6	46.3	9.2
		Milk	ND	5.1	49.1	11.5	104.5	11.7

[a] Relative standard deviation; [b] polystyrene; [c] not detected; [d] polyethylene terephthalate; [e] high-density polyethylene; [f] polypropylene

matrices such as milk and water, with recoveries ranging from 84.9 % to 101.2 % and RSDs below 7.3 %. For the first time, the impact of milk matrix composition (fat and protein) and environmental conditions on the release behavior of PAEs from MPs was investigated. The release of DMP decreased in milk compared to water, while BBP increased, highlighting the role of matrix polarity and DOM content in phthalate migration. Furthermore, accelerated aging of MPs showed a 2.8–4.5-fold increase in PAE release, particularly for BBP, confirming that photodegradation and UV exposure are critical factors influencing contaminant migration from plastics. Among the four real food-grade plastics tested, significant variation in PAE release was observed, with PS-based cream containers showing the highest levels (up to 195 ng mL^{-1} in milk). These results underscore the relevance of both plastic composition and matrix environment in PAE migration. Overall, this work provides a reliable and efficient extraction method for PAEs and highlights the potential health and environmental concerns related to PAEs release from aged and reused plastic food containers, particularly under varying environmental and matrix conditions.

Author Statement

Nasrin Moradi (NM), Delaram-Sadat Tavoussi-Shirazi (DT), Amir Mahdi Moshfegh (AM), Abuzar Kabir (AK) and Habib Bagheri (HB) contributed in the design and implementation of the research. NM (as the Ph.D student) performed the experiments and analyzed the data by the help of DT, the PhD student and Amir Mehdi Moshfegh (AM), as BSc student. HB (supervised) and AK (co-supervisor) coducted the project. All authors discussed the results and commented on the manuscript.

Also, NM and HB have contributed in writing and revising the article.

I confirm that the presented work is an original research that has not been published previously, and not under consideration for publication elsewhere, in whole or in part.

CRediT authorship contribution statement

Nasrin Moradi: Writing – original draft, Formal analysis, Data curation, Conceptualization. **Habib Bagheri:** Writing – review & editing, Supervision, Resources. **Amir Mahdi Moshfegh:** Data curation. **Delaram-Sadat Tavoussi-Shirazi:** Methodology. **Abuzar Kabir:** Writing – review & editing.

Declaration of Competing Interest

The authors declare that they have no known competing financial interests or personal relationships that could have appeared to influence the work reported in this paper.

Acknowledgment

This project was supported by the Graduate School and Research Office of Sharif University of Technology (Grant Number QA990417).

Appendix A. Supporting information

Supplementary data associated with this article can be found in the online version at doi:10.1016/j.jfca.2025.107764.

Data availability

All data regarding this manuscript are provided.

References

Abdar, A., Amiri, A., Mirzaei, M., 2022. Semi-automated solid-phase extraction of polycyclic aromatic hydrocarbons based on stainless steel meshes coated with metal–organic framework/graphene oxide. Microchem. J. 177, 107269–1072619. https://doi.org/10.1016/j.microc.2022.107269.

Abdar, A., Amiri, A., Mirzaei, M., 2023. Electrospun mesh pattern of polyvinyl alcohol/zirconium-based metal-organic framework nanocomposite as a sorbent for extraction of phthalate esters. J. Chromatogr. A 1707, 464295. https://doi.org/10.1016/j.chroma.2023.464295.

Acharya, S., Hu, Y., Abidi, N., 2021. Cellulose dissolution in ionic liquid under mild conditions: effect of hydrolysis and temperature. Fibers 9 (1), 5. https://doi.org/10.3390/fib9010005.

Alshehri, M.M., Ouladsmane, M.A., Aouak, T.A., ZA, A.L., Badjah Hadj Ahmed, A.Y., 2022. Determination of phthalates in bottled waters using solid-phase microextraction and gas chromatography tandem mass spectrometry. Chemosphere 304, 135214. https://doi.org/10.1016/j.chemosphere.2022.135214.

Amritha, P., Vinod, V., Harathi, P., 2022. A critical review on extraction and analytical methods of phthalates in water and beverages. J. Chromatogr. A 1675, 463175. https://doi.org/10.1016/j.chroma.2022.463175.

Aznar, M., Alfaro, P., Nerin, C., Kabir, A., Furton, K., 2016. Fabric phase sorptive extraction: An innovative sample preparation approach applied to the analysis of specific migration from food packaging. Anal. Chim. Acta 936, 97–107. https://doi.org/10.1016/j.aca.2016.06.049.

Behbahan, A.K., Mahdavi, V., Gordan, H., Bagheri, H., 2024. Fabrication of neem tree seed shell biochar polyamide composite for determination of pesticides in environmental water samples by GC-ECD: a comparison of various hard shell nuts' biochar in thin-film microextraction setup. J. Food Compos. Anal. 125, 105743. https://doi.org/10.1016/j.jfca.2023.105743.

Bhadange, Y.A., Carpenter, J., Saharan, V.K., 2024. A comprehensive review on advanced extraction techniques for retrieving bioactive components from natural sources. ACS Omega 9 (29), 31274–31297. https://doi.org/10.1021/acsomega.4c02718.

Cao, Y., Lin, H., Zhang, K., Xu, S., Yan, M., Leung, K.M., Lam, P.K., 2022. Microplastics: a major source of phthalate esters in aquatic environments. J. Hazard. Mater. 432, 128731. https://doi.org/10.1016/j.jhazmat.2022.128731.

Chen, Y., Wan, C., Liu, S., Wang, P., Zhang, G., 2021. A novel biomolecule and reactive flame retardant based on methionine for cotton fabrics. Cellulose 28, 11665–11678. https://doi.org/10.1007/s10570-021-04255-1.

Costa, R.S., Guedes, A., Pereira, A.M., Pereira, C., 2020. Fabrication of all-solid-state textile supercapacitors based on industrial-grade multi-walled carbon nanotubes for enhanced energy storage. J. Mater. Sci. 55 (23), 10121–10141. https://doi.org/10.1007/s10853-020-04709-0.

Ghoshal, T., Parmar, P.R., Bhuyan, T., Bandyopadhyay, D., 2023. Polystyrene foams: materials, technology, and applications. Polym. Foam.: Fundam. Types Foam. (Vol. 1) 121–141. https://doi.org/10.1021/bk-2023-1439.ch006.

Guadagno, L., Vertuccio, L., Naddeo, C., Calabrese, E., Barra, G., Raimondo, M., Sorrentino, A., Binder, W.H., Michael, P., Rana, S., 2019. Reversible self-healing carbon-based nanocomposites for structural applications. Polym. (Basel) 11 (5), 903. https://doi.org/10.3390/polym11050903.

Gulizia, A.M., Patel, K., Philippa, B., Motti, C.A., van Herwerden, L., Vamvounis, G., 2023. Understanding plasticiser leaching from polystyrene microplastics. Sci. Total Environ. 857 (Pt 1), 159099. https://doi.org/10.1016/j.scitotenv.2022.159099.

Hou, F., Chang, Q., Wan, N., Li, J., Zang, X., Zhang, S., Wang, C., Wang, Z., 2022. A novel porphyrin-based conjugated microporous nanomaterial for solid-phase microextraction of phthalate esters residues in children's food. Food Chem. 388, 133015. https://doi.org/10.1016/j.foodchem.2022.133015.

Huang, Z., Tu, C., Liu, H., Wang, L., Zhu, Z., Watanabe, I., 2020. Hollow fiber-solid phase microextraction of phthalate esters from bottled water followed by flash evaporation gas chromatography-flame ionization detection. J. Chromatogr. A 1619, 460953. https://doi.org/10.1016/j.chroma.2020.460953.

Kabir, A., Samanidou, V., 2021. Fabric phase sorptive extraction: a paradigm shift approach in analytical and bioanalytical sample preparation. Molecules 26 (4), 865. https://doi.org/10.3390/molecules26040865.

Kaur, R., Kaur, R., Grover, A., Rani, S., Malik, A.K., Kabir, A., Furton, K.G., 2019. Fabric phase sorptive extraction/GC-MS method for rapid determination of broad polarity spectrum multi-class emerging pollutants in various aqueous samples. J. Sep. Sci. 42 (14), 2407–2417. https://doi.org/10.1002/jssc.201900089.

Keshavarzi, M., Ghorbani, M., Mohammadi, P., Pakseresht, M., Ziroohi, A., Rastegar, A., 2022. Development of a magnetic sorbent based on synthesis of MOF-on-MOF composite for dispersive solid-phase microextraction of five phthalate esters in bottled water and fruit juice samples. Microchem. J. 182, 107934. https://doi.org/10.1016/j.microc.2022.107934.

Kumar, R., Malik, A.K., Kabir, A., Furton, K.G., 2014. Efficient analysis of selected estrogens using fabric phase sorptive extraction and high performance liquid chromatography-fluorescence detection. J. Chromatogr. A 1359, 16–25. https://doi.org/10.1016/j.chroma.2014.07.013.

Li, B., Zhong, Q., Li, D., Xu, K., Zhang, L., Wang, J., 2018. Influence of ethylene glycol methacrylate to the hydration and transition behaviors of thermo-responsive interpenetrating polymeric network hydrogels. Polym. (Basel) 10 (2), 128. https://doi.org/10.3390/polym10020128.

Li, Y., Liu, C., Yang, H., He, W., Li, B., Zhu, X., Liu, S., Jia, S., Li, R., Tang, K.H.D., 2024. Leaching of chemicals from microplastics: A review of chemical types, leaching mechanisms and influencing factors. Sci. Total Environ. 906, 167666. https://doi.org/10.1016/j.scitotenv.2023.167666.

Liu, X., Shi, H., Xie, B., Dionysiou, D.D., Zhao, Y., 2019. Microplastics as both a sink and a source of bisphenol a in the marine environment. Environ. Sci. Technol. 53 (17), 10188–10196. https://doi.org/10.1021/acs.est.9b02834.

Lu, C., Lin, F., Shao, H., Bi, S., Chen, N., Shao, G., Jiang, J., 2022. Carboxylated carbon nanotube/polyimide films with low thermal expansion coefficient and excellent mechanical properties. Polym. (Basel) 14 (21), 4565. https://doi.org/10.3390/polym14214565.

Maity, D., Rajavel, K., Rajendra Kumar, R.T., 2021. MWCNT enabled smart textiles based flexible and wearable sensor for human motion and humidity monitoring. Cellulose 28, 2505–2520. https://doi.org/10.1007/s10570-020-03617-5.

Moradi, N., Soufi, G., Kabir, A., Karimi, M., Bagheri, H., 2023. Polyester fabric-based nano copper-polyhedral oligomeric silsesquioxanes sorbent for thin film extraction of non-steroidal anti-inflammatory drugs. Anal. Chim. Acta 1270, 341461. https://doi.org/10.1016/j.aca.2023.341461.

Olayanju, B., Kabir, A., Furton, K.G., 2024. Development of a universal sol–gel sorbent for fabric phase sorptive extraction and its application in tandem with high performance liquid chromatography-ultraviolet detection for the analysis of phthalates in environmental and drinking water samples. Microchem. J. 196, 109619. https://doi.org/10.1016/j.microc.2023.109619.

Paluselli, A., Fauvelle, V., Galgani, F., Sempere, R., 2019. Phthalate release from plastic fragments and degradation in seawater. Environ. Sci. Technol. 53 (1), 166–175. https://doi.org/10.1021/acs.est.8b05083.

Roy, D., Ye, A., Moughan, P.J., Singh, H., 2020. Composition, structure, and digestive dynamics of milk from different species—A review. Front. Nutr. 7, 577759. https://doi.org/10.3389/fnut.2020.577759.

Senathirajah, K., Attwood, S., Bhagwat, G., Carbery, M., Wilson, S., Palanisami, T., 2021. Estimation of the mass of microplastics ingested–a pivotal first step towards human health risk assessment. J. Hazard. Mater. 404, 124004. https://doi.org/10.1016/j.jhazmat.2020.124004.

Tartaglia, A., Covone, S., Rosato, E., Bonelli, M., Savini, F., Furton, K., Gazioglu, I., D'Ovidio, C., Kabir, A., Locatelli, M., 2022. Fabric phase sorptive extraction (FPSE) as an efficient sample preparation platform for the extraction of antidepressant drugs from biological fluids. Adv. Sample Prep. 3, 100022. https://doi.org/10.1016/j.sampre.2022.100022.

Torabi, E., Abdar, A., Lotfian, N., Bazargan, M., Simms, C., Moussawi, M.A., Amiri, A., Mirzaei, M., Parac-Vogt, T.N., 2024. Advanced materials in sorbent-based analytical sample preparation. Coord. Chem. Rev. 506, 215680. https://doi.org/10.1016/j.ccr.2024.215680.

van 't Erve, T.J., Rosen, E.M., Barrett, E.S., Nguyen, R.H.N., Sathyanarayana, S., Milne, G. L., Calafat, A.M., Swan, S.H., Ferguson, K.K., 2019. Phthalates and phthalate alternatives have diverse associations with oxidative stress and inflammation in pregnant women. Environ. Sci. Technol. 53 (6), 3258–3267. https://doi.org/10.1021/acs.est.8b05729.

Xia, B., Sui, Q., Du, Y., Wang, L., Jing, J., Zhu, L., Zhao, X., Sun, X., Booth, A.M., Chen, B., Qu, K., Xing, B., 2022. Secondary PVC microplastics are more toxic than primary PVC microplastics to Oryzias melastigma embryos. J. Hazard. Mater. 424 (Pt B), 127421. https://doi.org/10.1016/j.jhazmat.2021.127421.

Yan, Y., Zhu, F., Zhu, C., Chen, Z., Liu, S., Wang, C., Gu, C., 2021. Dibutyl phthalate release from polyvinyl chloride microplastics: Influence of plastic properties and environmental factors. Water Res 204, 117597. https://doi.org/10.1016/j.watres.2021.117597.

Yang, Q., Wu, Y., Zhang, S., Xie, H., Han, D., Yan, H., 2025. Recent advancements in the extraction and analysis of phthalate acid esters in food samples. Food Chem. 463 (Pt 2), 141262. https://doi.org/10.1016/j.foodchem.2024.141262.

Yu, Y., Kumar, M., Bolan, S., Padhye, L.P., Bolan, N., Li, S., Wang, L., Hou, D., Li, Y., 2024. Various additive release from microplastics and their toxicity in aquatic environments. Environ. Pollut. 343, 123219. https://doi.org/10.1016/j.envpol.2023.123219.

Yue, Q., Huang, Y.-Y., Shen, X.-F., Yang, C., Pang, Y.-H., 2020. In situ growth of covalent organic framework on titanium fiber for headspace solid-phase microextraction of 11 phthalate esters in vegetables. Food Chem. 318, 126507–1265017. https://doi.org/10.1016/j.foodchem.2020.126507.

Zha, F., Shang, M., Ouyang, Z., Guo, X., 2022. The aging behaviors and release of microplastics: a review. Gondwana Res 108, 60–71. https://doi.org/10.1016/j.gr.2021.10.025.